CrossMark

Phosphorus Budget of the Sundarban Mangrove Ecosystem: Box Model Approach

R. Ray[1,2] · N. Majumder[1] · C. Chowdhury[1] · S. Das[1] · T. K. Jana[1]

Abstract Phosphorus (P) cycling in mangroves plays an important role in productivity but the magnitude of atmospheric input in the mangrove P budget is still uncertain. This study applied a box model approach to assess P budget in the Indian Sundarban, the world's largest mangrove ecosystem for conceptual understanding of P cycling and for better representation of transport and transformation of P within the mangrove ecosystem. The P content in the sediment (0.19–0.67 μg g^{-1}) was found much below its maximum retention capacity (322 μg g^{-1}) and was lower than the mean marine sediment (669 μg g^{-1}). The C:N and C:P ratios were correlated ($r^2 = 0.66$, $P < 0.01$) and the major fraction of available P was recycled within the organic structure of mangrove ecosystem, thus maintaining productivity through conservation strategies. Atmospheric input accounted for 56.7% of total P input (16.06 Gg year^{-1}) and 50% of total P output (14.7 Gg year^{-1}) was attributed to plant uptake. Budget closing or unaccounted P (1.36 Gg) was only 8.5% of the total input. Two feedback pathways, i.e., input of P from dust fallout and biochemical mineralization of organic matter, significantly affected P availability. The findings of the study suggest that atmospheric deposition is of major importance as a natural and/or anthropogenic forcing function in the Sundarban mangrove system.

Communicated by Marianne Holmer

✉ R. Ray
raghab.ray@gmail.com; raghab.ray@univ-brest.fr

[1] Department of Marine Science, University of Calcutta, 35, B. C. Road, Kolkata 700019, India

[2] Laboratoire des Sciences de l'Environnement Marin (LEMAR), UMR 6539 (UBO/CNRS/IRD/Ifremer), Institut Universitaire Europeen de la Mer, rue Dumont d'Urville, 29280 Plouzane, France

Introduction

Investigation on carbon–nutrient interactions has important implications for the prediction of future carbon uptake and storage in tropical ecosystems and global climate change (Yang et al. 2014). In low land tropical soil, limited availability of parent phosphorus (P) materials to provide fresh P input through weathering (Yang and Post 2011) and prevalence of kaolinite, aluminum, and iron oxide/hydroxides that effectively sorb P (Sanchez 1977) result in strong P limitation for tropical ecosystems (Wright et al. 2011), leading to ecosystem retrogression (Peltzer et al. 2010). Phosphates move quickly through plants and animals; however, the processes governing their movement through the soil or ocean are very slow and make the phosphorus cycle overall one of the slowest biogeochemical cycles (Oelkers 2008). However, the absence of gaseous phases makes P cycle relatively simple in nature. Soil phosphorus release to surface runoff and to subsurface flow is a complex interaction between the type of P input, soil type and management, and transport processes (Branom and Sarkar 2004; Schelde et al. 2006). Human interference in the P cycle occurs by overuse or careless use of phosphorus fertilizers that results in eutrophication in the water part, thus inducing anoxic conditions (Conley et al. 2009).

Phosphate-P in tropical forests can be immobile and unavailable for plant use due to their occurrence in geochemically protected forms, i.e., P either associated with iron/aluminum/calcium hydroxides or can be adsorbed onto mineral surfaces or protected within mineral matrices or present in organic compounds (Ruttenberg 1992; Cross and Schlesinger 1995; Johnson et al. 2003); thus, organisms that

solubilize P can have important implications for plant growth, especially in nutrient-limited environments.

Mangrove swamps are a common feature covering 60–70% of tropical and subtropical intertidal regions of coastal environment (FAO 2004) and are highly productive (Alongi 2009; Clark et al. 2001) and most rich in carbon in tropics (Donato et al. 2011). Mangrove swamps are rich in recycled nutrients that are mainly derived from litter decomposition (Alongi et al. 1989; Holguin et al. 2001; Ray et al. 2014). However, mangroves are often limited by the availability of micro- and macronutrients specially N and P, mainly due to high nutrient use efficiency for developing cell walls (Alongi et al. 1992; Lovelock et al. 2005; Reef et al. 2010). Many mangrove environments tend to be nutrient limited and that, in general, tropical soils will be less fertile, particularly in P, which in contrast to N cannot be replaced through biological fixation (Reich and Oleksyn 2004; Lovelock et al. 2007). Mangrove biogeochemistry of plant and sediment derived phosphorus focus on the large, slow moving chemical reservoirs and their smaller but more active exchange or cycling either driven by biological activity in the mangrove reservoirs. Occurrence of phosphate-solubilizing bacteria (PSB) in association with mangrove roots (Vazquez et al. 2000; Kothamasi et al. 2006) serves an important role in P availability to plant (Dick et al. 2000; Kothamasi et al. 2006; Das et al. 2014). Its involvement in a range of processes, i.e., solubilization and remobilization (Oberson et al. 2001; Oehl et al. 2001), affect the dynamics and transformation of soil phosphorus and are thus an integral part of the P cycle (Gerretsen 1948). Mangrove swamps suffer from many of the environmental disturbances like deforestation (Hussein 1995; Kelleher et al. 1995; Spalding et al. 1997; Valiela et al. 2001), land reclamation (Terchunian et al. 1986; Primavera 1997; Singh et al. 2015), garbage and sewage dumping, and dredging and damming of rivers (Wolanski 1992). Such events could result in transition of biological P cycling to more of geochemical processes in tropical mangrove ecosystems (Dittmar and Lara 2001; McGrath et al. 2001). Thus, it is of interest to study at different trophic levels and a range of spatio-temporal scales to identify biocomplexity and overall functioning of the mangrove ecosystem (Feller et al. 2010). The major pools of P are live biomass (above ground and below ground) and sediment. P input within mangrove ecosystem is driven by various processes such as atmospheric dry and wet deposition, canopy nutrient transfer, litter fall, organic matter mineralization in sediment, and anthropogenic activities (sewage, agriculture, aquaculture, etc.) (Ramos et al. 2007).P cycling in mangroves plays an important role in productivity, yet complete ecosystem scale budgets are rare, particularly in tropical Sundarban mangrove ecosystem, which is known for high CO_2 sequestration, litter fall, and biodiversity (Ray et al. 2011; Dey et al. 2012; Chowdhury et al. 2012).

Therefore, our aim is to develop a P budget for the Sundarban mangrove ecosystem, using a box model approach that incorporates stocks and fluxes including litterfall, deposition, plant uptake, aerosol emission, tidal exchange, above- and below-ground biomass, and sediment stocks. This study will provide the basic data for conceptual understanding of P cycling and for better representation of transport and transformation of P within the mangrove ecosystem.

Materials and Methods

Study Area

The study sites were located in the Indian Sundarban, which is part of the estuary associated with the River Ganges, on the northeast coast of the Bay of Bengal. In 1985, the Indian Sundarban was included in UNESCO's list of world heritage site, and in 1989, India designated 9360 km^2 of Sundarban as a biosphere reserve, which are subdivided into forest (4264 km^2) and aquatic (1781 km^2) sub-ecosystems. The area is covered with thick mangroves harboring 34 true mangrove species such as *Avicennia alba*, *A. marina*, *A. officinalis*, *Ceriops decandra*, *Xylocarpus granatum*, *Aegialitis rotundifolia*, *Bruguiera gymnorrhiza*, *Aegiceras corniculatum*, *Sonneratia apetala*, *Excoecaria agallocha*, and *Heritiera fomes*. Mangrove plants rarely exceed 10 m in height, and the over-forest trajectory of the wind (fetch) is about 15 km.

Field work was conducted during the period between September 2009 and March 2011 at five sites (Lothian Island North, Stn.1; Lothian Island South, Eco Camp, Stn.2; Prentice Island, Stn.3; Bonnie camp,Stn.4; and Halliday Island, Stn.5) (21° 32′ and 22° 40′ N; 88° 50′ and 89° E) (Fig. 1). These five stations were selected from virgin forest: three are from west Sundarban (Stn.1, Stn.2, and Stn.3) and other two were from east Sundarban (Stn.4 and Stn.5). These islands are almost free from both direct and indirect human interferences and are fully covered by different mangrove vegetation. Islands are criss-crossed by many tidal creeks and vegetation is comparatively denser on either side of the creeks with comparable geomorphological features. *Avicennia marina* and *Avicennia alba* are the dominant mangrove species at Stns.1, 2, and 3 followed by patches of *Aegialitis rotundifolia*, *Excoecaria agallocha*, and *Bruguiera gymnorrhiza*. At Stns.4 and 5, *Avicenia marina* with few patches of *Aegiceras corniculatu*, *Agialites rotundifolia*, and *Phoenix paludosa* are more common. The sediment of these islands is typically muddy and alluvial in nature. These islands are periodically inundated and exposed with tide and are considered as representative of the Sundarban mangrove forest.
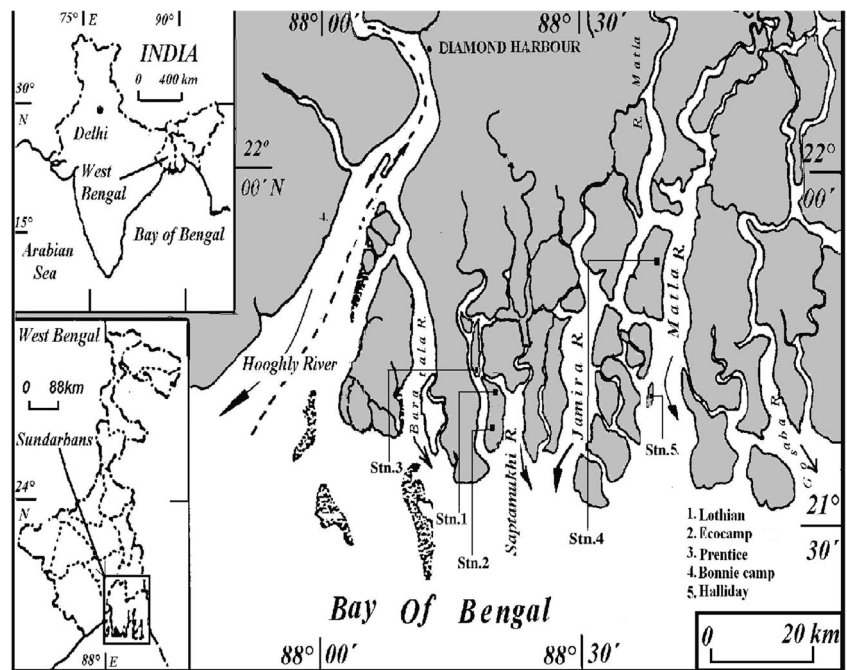
Biomass and Litter

For more details about climate, ecogeography, hydrodynamics, biodiversity of the sites, and methodology for estimation of above-ground biomass (AGB), below-ground biomass (BGB), litter fall, and sediment samples, refer to Ray et al. (2011, 2014). Briefly, quadrates (100 m × 10 m) were selected randomly at five stations for monthly observations and AGB and BGB were estimated using allometric equations:

$$\text{AGB} = 1.0471 \, d^{0.864} H^{0.635} \rho^{-1.37} \left(r^2 = 0.99, p < 0.001, n = 100\right)$$
$$\text{BGB} = \text{AGB}^{1.63}/30.29 \qquad \left(r^2 = 0.97, p \; < 0.001, n = 100\right)$$

where d = diameter of breast height in centimeters, H = tree height in meters, and ρ = wood density in grams per cubic centimeter derived by Ray et al. (2011). Monthly increment of cbh (circumference at breast height) was recorded for 389 trees/500 m^2 and the integrated value was considered to estimate the net accumulation of P as AGB and BGB. Core samples were collected by using a corer made of stainless steel (5.5 cm inner diameter) at different depths, and sediment-P stock was calculated from bulk density (ρ = 2.56 g cm^3) and the P% at each depth in the sediment profile of 0–60 cm. Litter were collected using traps (3 × 3 m) placed randomly inside the deep mangrove forest. All samples (AGB, BGB, litter, and sediment) were oven-dried at 60 °C for the determination of P content. Plant-P stock and its sequestration to forest biomass were estimated from its concentration in dry biomass of different plant parts (leaf + stem + root). P stock (plant and sediment) and different fluxes (litter fall as F_{Litt} and plant uptake as F_{uptake}) were expressed in Kg P ha^{-1} and μmol cm^{-2} day^{-1}, respectively.

Dry Deposition

Aerosol is a system of solid or liquid particles suspended by a mixture of gases. The term aerosol covers a wide spectrum of particles, like coarse (air-borne dust with aerodynamic diameter > 10 μm) and fine mode particles (like sea salt particles, carbon black dust, pollen, and many others with aerodynamic diameter < 10 μm). Dry deposition of these particles is size dependent and coarse particles with deposition velocity > 1 cm s^{-1} falls out quickly (Graedel and Crutzen 1993). No single instrument could measure particles over the entire range. A combination of techniques was used for aerosol measurements. In the present study, cascade impactors for fine mode and Mylar strips coated with grease were used as the collection surface (10.26 cm^2) for the coarse mode.

Air-Borne Dust with Aerodynamic Diameter > 10 μm

A knife-edge surrogate surface (KSS) made of polyvinyl chloride sheet with mounted Mylar strips (Graphic Arts Systems Cleveland, USA) coated with 2–3 mg of Apezion L grease was used as the collection surface (10.26 cm^2) for the particles. Sampling was carried out in the dry season from the month of January to the month of May (151 days). Samples were collected twice a month for 24 h. The mass of deposited particles was obtained by the difference between the initial and final weight of Mylar

strips. All of the grease from Myler strips was extracted using hexane to collect particles from the strip. Hexane was evaporated and residue was extracted with deionized water following sonication at 60 °C for 3 h. The solutions were then filtered and were analyzed for phosphate using ion chromatography (Metrohm, 792 Basic IC). Dust deposition fraction of P ($\mu g\ m^2\ s^{-1}$) was estimated by dividing the deposited amount with area of collection and duration of samples.

Aerosol with Aerodynamic Diameter < 10 μm

Size-segregated aerosol samples were collected during dry season (January to May, 151 days) on the quartz fiber substrate using a cascade impactor (flow rate $1.7\ m^3\ h^{-1}$) fitted with a preseparator (Pacwill Environmental, Canada), and total aerosol mass was measured by weighing the substrate, before and after sampling using a microbalance (Metler AE 240) in a controlled environment chamber maintained at a temperature of 23 ± 2 °C and relative humidity of $35 \pm 5\%$. Water-soluble inorganic PO_4^{-3} was extracted by ultrasonic agitation using 20 mL deionized water for 20 min. The extracts were filtered through a nylon membrane filter paper and kept in the prewashed polypropylene bottles. Chemical analyses for the water-soluble inorganic ions were conducted by Ion Chromatography (Metrohm 792 basic IC) using separator columns (Metrosep Supp 3 (6.1005.320)) for anion analysis, fitted with a guard column (PRP-1 IC guard column cartridge (6.1005.050)).

Dry deposition of aerosol was determined from concentration of different size fractions measured by each impactor stage and deposition velocity of particle for each impactor stage. For more details about dry deposition velocity, refer to Sehmel and Hodgson (1978) and Chatterjee et al. (2006).

Emission of Aerosol

Emissions of aerosol ($\mu g\ m^{-2}\ s^{-1}$) was estimated by dividing an atmospheric concentration of $\chi\ \mu g\ m^{-2}$ and average wind speed of u (0.36–5.74 m s^{-1} at 10 m) over the phase distance X (up to 10 km) (Gifford and Hanna 1973) with C (= 0.7979 X/σz (1 - b) and σz = aXb) as described elsewhere (Chatterjee et al. 2006). Here, a and b for different atmospheric dispersion conditions are compared according to Pasquill and Smith (1983). Micrometeorological parameters were recorded by a computerized weather station (Model: Davis 7440). For estimating the emission fraction of P, a distributed area source was considered in which the water surface (1781 km^2, 10,686 × 10^6 m^3) contributions were treated as coming from a continuous distribution of infinitesimal sources.

Sediment and Tidal Water

Redox potential (Eh) and pH were measured in situ by lowering electrodes into the sediment section (Vischer et al. 1991; Fiedler et al. 2003). Texture analysis of air-dried sediment was carried out following the pipette method (Piper 1950) and porosity was calculated from the different percentages of clay, silt, and sand (Knab et al. 2009). Pore water was separated from sediment by means of centrifugation (30 min, 5000 rpm). Salinity was determined by Mohr–Knudsen titration. The C, N in dried sediment, and plant materials were measured by CHN Analyzer (2400 series-11, Perkin-Elmer). Sediment and the filtered particulate matter samples were digested with a mixture of nitric, hydrochloric, hydrofluoric, and perchloric acid (Sturgeon et al. 1982), and P content was determined by the spectrophotometric method (Chang and Jackson 1957; APHA 1995).

Tidal water samples (low and high tide) were collected by Niskin bottles from the estuarine surface, filtered (0.45 μm millipore) and analyzed afterwards for the estimation of total phosphate (P) and nitrogen (N) following the standard method of Grasshoff (1983) by spectrophotometer (Systronics, UV–VIS Spectrophotometer, 117). Pore water nutrients were also measured following the same method. Relative accuracy error of $\pm 3\%$ for nitrate and nitrite, $\pm 5\%$ for ammonia, and $\pm 2\%$ for phosphate was achieved. The detection limits were 0.1 μM for dissolved inorganic nitrogen (DIN) and 0.05 μM for dissolved inorganic phosphate (DIP). Total phosphorus (organic and particulate) was obtained by difference subtraction of filtered and unfiltered seawater samples, after acid persulphate oxidation.

Quantification of Phosphate-Solubilizing Bacteria

To quantify phosphate-solubilizing bacteria (PSB), the 60-cm sediment core was sectioned into 2-cm segments. For each sampling sites (upper, middle, and lower littoral zones), the sediment corresponding to the same depth was pooled and 10 g sample was homogenized in sterile phosphate buffer. Serial dilutions up to 10–4 were made and inoculation was done with 0.1 mL PSB in a selective medium named Pikovskaya's medium which had the following composition: glucose (10 g), $Ca_3(PO4)_2$ (5 g), $(NH4)_2SO_4$ (0.5 g), KCl (0.2 g), agar (20 g), isotonic solution with the sediment prepared from NaCl and sterilize distilled water (1 L), and pH maintained at (6.8–7.0) (Ramanathan et al. 2008; Das et al. 2014). Pikovskaya's medium allows the growth of only PSB among the other group of microbes like cellulose-degrading bacteria, sulfate-reducing bacteria, nitrifying bacteria, and nitrogen-fixing bacteria. Again, the colony of PSB was easily recognized and enumerated with a clear zone around their colony as PSB produces acids that dissolute calcium triphosphate used in that Pikovskaya's medium.

Diffusive and Advective P Flux Estimations

Diffusive P fluxes (μmol m^{-2} day^{-1}) were calculated using the following equation (Berner 1980): $F_{Diff} = -\varphi\,Ds(\delta C/\delta Z)_{Z=0}$, where F_{Diff} is the diffusive flux, φ is the porosity of the sediment (0.7, Ray et al. 2014), Ds is the whole sediment diffusion coefficient (cm^2 s^{-1}) obtained from the following formula (Iversen and Jorgensen 1993): Ds = $D_0/1 + n(1-\varphi)$, where D_0 is the free solution diffusion coefficient, and $n = 3$ (Knab et al. 2009). The concentration gradient at zero depth, $(\delta C/\delta Z)_{Z=0}$, was estimated by linear regression between concentrations and depths.

Advective P fluxes (F_{adv}) from intertidal forest sediment to the estuarine water column were estimated by using the following relation (Reay et al. 1995): $F = \Phi \times \nu \times C$, where Φ = porosity of sediment, ν = average linear velocity = d/Φ (d = specific discharge), and C = pore water P concentration. In the end of the calculation, Φ is nullified. The specific discharge (9.6 ± 1.7 cm day^{-1} or cm^3 cm^{-2} day^{-1}, Dutta et al. 2015) for the intertidal sediment was recorded by measuring the rate of accumulation of pore water in an excavated pit of known surface area during low tide.

Sedimentation flux of particulate P (F_{part}) was estimated by multiplying the particulate P concentration with the mass accumulation rate (0.41–0.78 g cm^{-2} year^{-1}, Banerjee et al. 2011).

For the estimation of river input and coastal exchange of P, land ocean interactions in the coastal zone (LOICZ) approach (Gordon et al. 1996, Mukhopadhyay et al. 2006) was used for the mangrove-dominated estuarine system. Residual flow ($V_R = V_Q + V_P - V_E$) and exchange flow [$V_X = V_R \times S_R/(S_{estuary} - S_{ocean})$] were calculated from fresh water inflow (V_Q), precipitation (V_P), evaporation (V_E), and salinity of the out flowing water (S_R = average salinity of the system and adjacent seawater, $S_R = (S_{estuary} + S_{ocean}) / 2$). Using mean P concentration during high tide and low tide, river runoff (V_Q P_{river}), residual flow [$V_R(P_{estuary} + P_{ocean}) / 2$], and exchange flow [$V_x(P_{estuarine} - P_{ocean})$] were calculated for the monsoon and non-monsoon periods.

Statistical Analysis

Statistical analysis was performed by MINITAB (version 13.1) statistical software package. Any doubtful data was tested using the Q test. The ratio Q was calculated by arranging the data in decreasing order of numbers, and the difference between the suspect number and its nearest neighbor was divided by the difference between the highest and lowest number. The ratio was compared with tabulated values of Q at the 95% confidence level (Christian 2001). A one-way analysis of variance (ANOVA) and t test were employed to test differences of data among stations.

Results

Seasonal variations of physico-chemical properties of sediment and water are given in (Table 1). Mangrove ecosystems were influenced by seasonal changes in temperature (winter,

Table 1 Summary of physico-chemical properties of mangrove sediment (dry weight basis, nmol g^{-1}) and pore water and tidal water nutrients (μM). PSB = phosphate-solubilizing bacteria, TEP = total exchangeable PO$_4$-P, DIN = dissolve inorganic nitrogen (NO$_3$ + NO$_2$ + NH$_4$) averaged for each season during the study period (mean ± SD, $n = 48$)

Parameters	Pre-monsoon	Monsoon	Post-monsoon
pH	8.23 ± 0.05	7.72 ± 0.22	8.21 ± 0.04
Salinity (pore water)	30.0 ± 2.5	18.9 ± 1.2	20.5 ± 1.5
Eh (mv)	− 45.45 ± 119	− 78.37 ± 59.0	− 70.64 ± 65.8
Org-C (%)	0.85 ± 0.12	0.75 ± 0.10	1.11 ± 0.18
PSB (C.F.U × 10^6 g^{-1})	0.77 ± 0.25	0.91 ± 0.22	1.09 ± 0.28
TEP			
Sediment	9.77 ± 0.97	8.03 ± 1.3	16.5 ± 3.4
Pore water	1.1 ± 0.3	1.62 ± 0.05	0.78 ± 0.08
Tidal water	0.59 ± 0.33	0.95 ± 0.15	0.46 ± 0.17
DIN			
Sediment	206 ± 70	133 ± 41	325 ± 58
Pore water	4.84 ± 1.5	4.93 ± 2.5	4.7 ± 1.9
Tidal water	18.85 ± 2.5	24.11 ± 2.8	21.91 ± 1.8
Sediment texture			
Sand %	6.0 ± 0.57	5.0 ± 1.4	16.0 ± 4.1
Silt %	80.0 ± 5.3	87.0 ± 4.3	72.0 ± 5.1
Clay %	14.0 ± 1.1	8.0 ± 1.3	12.0 ± 3.5
Porosity	0.7	0.7	0.7
Diffusion constant (cm^2 s^{-1})	9.26 × 10^{-6}	9.26 × 10^{-6}	9.26 × 10^{-6}

Phosphate conc. (nmol g^{-1} drywt.)

PSB C.F.U (x10^6 g^{-1} drywt.)

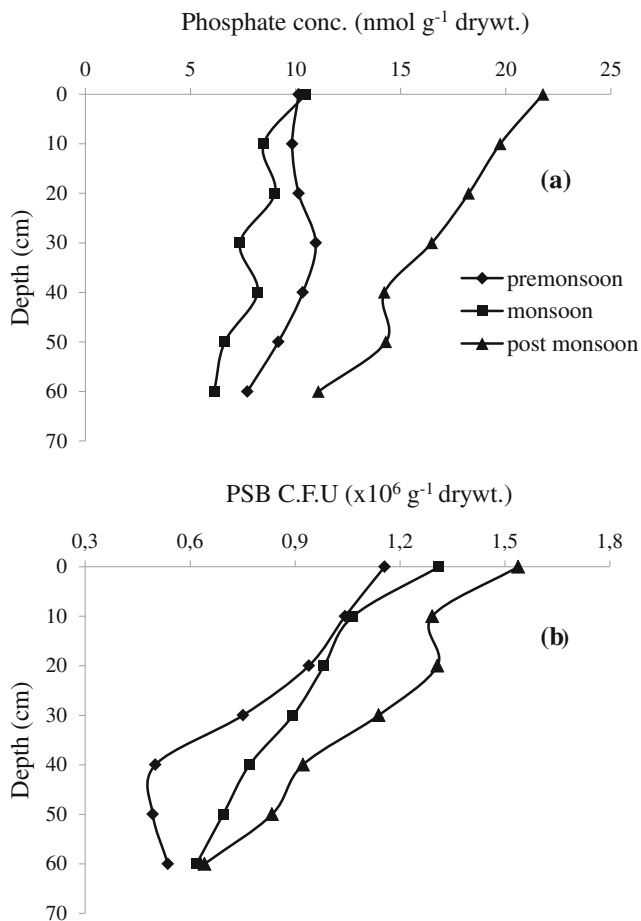**Fig. 2** Down-core seasonal variations of **a** phosphate concentration and **b** phosphate-solubilizing bacteria (PSB) count

Table 2 Seasonal variations of elemental C, N, P, and their molar ratios in different mangrove parts and sediments (avg. up to 60 cm depth)

Dry wt%	Pre-monsoon	Monsoon	Post-monsoon
Living leaf			
C%	46.47 ± 3.5	46.62 ± 3.2	46.92 ± 2.8
N%	1.84 ± 0.45	1.84 ± 0.45	1.85 ± 0.45
P%	0.10 ± 0.03	0.10 ± 0.02	0.09 ± 0.02
C:N:P	1200:40:1	1204:40:1	1338:29:1
Leaf litter			
C%	40.01 ± 2.6	41.32 ± 2.4	42.84 ± 2.0
N%	1.17 ± 0.08	1.18 ± 0.11	1.18 ± 0.09
P%	0.11 ± 0.09	0.12 ± 0.12	0.12 ± 0.16
C:N:P	940:35.5:1	889:39:1	922:22:1
Stem			
C%	42.42 ± 0.4	42.88 ± 0.4	42.98 ± 0.3
N%	1.02 ± 0.09	1.02 ± 0.1	1.02 ± 0.12
P%	0.08 ± 0.01	0.09 ± 0.03	0.09 ± 0.01
C:N:P	1369:28:1	1230:25:1	1233:25:1
Root			
C%	44.98 ± 1.3	44.81 ± 1.1	43.37 ± 1.1
N%	1.17 ± 0.08	1.19 ± 0.16	1.21 ± 0.13
P%	0.10 ± 0.03	0.11 ± 0.02	0.12 ± 0.01
C:N:P	1162:26:1	1052:24:1	934:22:1
Sediment			
C%	0.85 ± 0.12	0.75 ± 0.10	1.11 ± 0.18
N%	0.045 ± 0.01	0.061 ± 0.01	0.072 ± 0.00
P%	0.012 ± 0.0	0.024 ± 0.0	0.033 ± 0.0
C:N:P	183:8.3:1	81:5.6:1	87:4.8:1

19.1 ± 4 °C versus monsoon and non-monsoon, 29.1 ± 2 °C) and mean salinity ($S_{estuary}$, 19 psu versus S_{ocean}, coastal water, 31 psu). Suspended particulate matter concentration ranged from 50 ± 12 mg L^{-1} in the non-monsoon to 150 ± 35 mg L^{-1} in the monsoon. Sediment textural analysis showed that silt (72–87%) was the major component of sediment followed by 5–16% sand and 8–14% clay (Table 1). Total organic carbon in sediments exhibited a greater concentration in the post-monsoon compared to other times of the year. Average concentration of inorganic nitrogen (190 ± 50 nmol g^{-1} d.w.) was greater than phosphorus (11.4 ± 3.6 nmol g^{-1} d.w.) with N:P ratio of 17. Down-core phosphate and PSB profile (Fig. 2a, b) exhibited an overall decreasing trend with depth. Maximum average population of PSB (1.53 CFU × 10^6 g^{-1} dry wt. of sed.) was found during the non-monsoon from the surface sediment and minimum was found during the monsoon (0.55 CFU × 10^6 g^{-1} dry wt. of sed.) at 60 cm of depth.

A seasonal trend was a common feature for physicochemical parameters and all stations showed lower salinity, pH, N, and P in sediment and greater N and P in tidal and pore water during the monsoon compared to the other time of the year (*t* test $P < 0.05$–0.10).

Above Ground (AGB-P), Below Ground (BGB-P), and Sediment-P

The allocation of C, N, and P among different components of mangroves is given in Table 2. AGB-P was increased from 75.52 to 99.45 Kg P ha^{-1} and BGB-P from 26.19 to 40.86 Kg P ha^{-1} (Fig. 3). Spatial variation of AGB-P, BGB-P, and sediment-P stock showed the highest level at Halliday Island (Stn.5. 122.5, 63.5 Kg P ha^{-1}) and the lowest at Eco Camp (Stn.2, 64.7, 13.09 Kg P ha^{-1}) (Fig. 4). The mean AGB-P, 99.9 ± 22.5 Kg P ha^{-1}, was found 2.8 times greater than BGB-P with coefficient of variance (CV) of 22.5% for AGB-P and 57% for BGB-P. Phosphorus stock in the sediment (expressed as depth integrated value) ranged from 3.19 to 4.86 Kg P ha^{-1} across stations with an average stock of 4.08 ± 0.67 Kg P ha^{-1} and CV of 16.4%.

To find how much of the variation in our measurements of AGB-P, BGB-P was due to between sample differences and how much due to random variability within the samples, ANOVA test was applied. Observed value of *F* was 0.23 versus the critical value of *F* 2.13 with (10, 33) degrees of

Fig. 3 Monthly variation of phosphorus stock in the above-ground biomass (AGB-P), below-ground biomass (BGB-P), and sediment
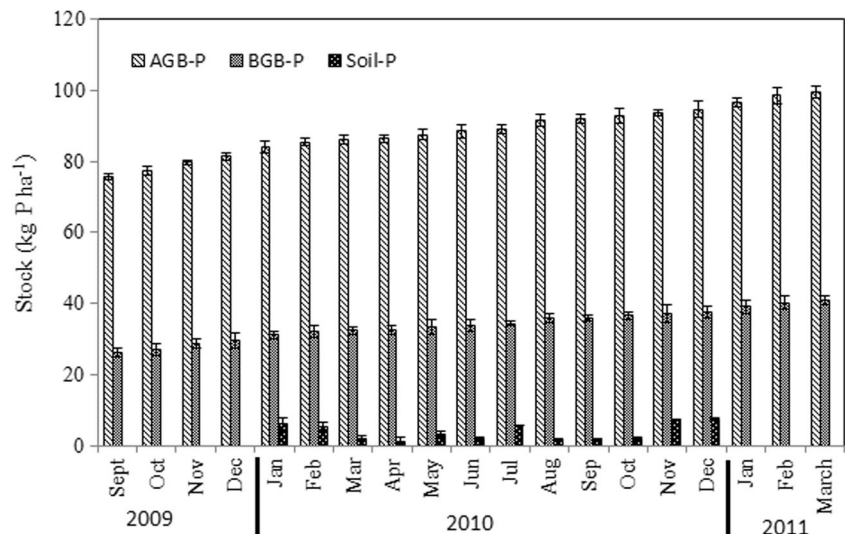
freedom at $P = 0.05$, indicating that the difference of observed parameters at different sites was insignificant.

Litter P

Average concentrations of P in litters (0.11–0.12%) of mainly *Avicennia* mangroves were similar in three seasons (Table 2). Litter fall showed monthly variation and average F_{Litt-P} was 126.2 ± 78.7 µmol m^{-2} day^{-1}. The highest (364 µmol m^{-2} day^{-1}) and lowest (72.36 µmol m^{-2} day^{-1}) values of F_{Litt-P} occurred in December and July, respectively (Fig. 5), with 62.3% coefficient of variance.

Flux Estimates

The depth profile of P in the sediment (Fig. 2a) indicates its downward diffusion and the diffusion coefficient (Ds) for the

sediment column was calculated to be 9×10^{-6} cm^2 s^{-1} for the sediment with density of 2.56 g cm^{-3}. From the concentrations of P in pore water (0.78–1.68 µM) and in suspended particulate matter (0.2 µM), total advective and sedimentation fluxes of P were estimated at 3.61 and 0.78 Gg P year^{-1}, respectively. Diffusive P flux varied between 0.22 and 3.47 µmol m^{-2} day^{-1} (Fig. 5) or 0.06 Gg P year^{-1}.

The amount of fresh water flowing (V_Q) into the estuarine system was estimated to be 72.5×10^9 m^3 and about 58% occurred during the monsoon (mid June to mid October). Annual rain fall (V_P) and evaporation from the water surface (V_E, in m^3) were calculated to be 8.4×10^9 and 5.4×10^9, respectively. Net residual flows (V_R) of 50.58×10^9 and 24.96×10^9 m^3 and the exchange flow (V_X, m^3) of 105.36×10^9 and 52.0×10^9 m^3 were found during the monsoon and non-monsoon periods, respectively. Mean P concentration (µM) increased from 0.78 (non-monsoon) to 1.17

Fig. 4 Spatial variations of plant-P (AGB-P, BGB-P) and sediment-P stock in the Sundarbans
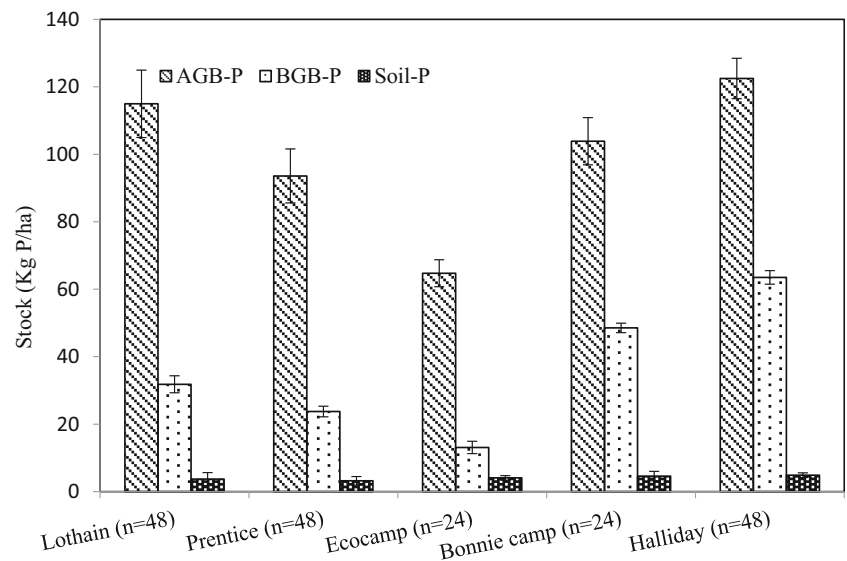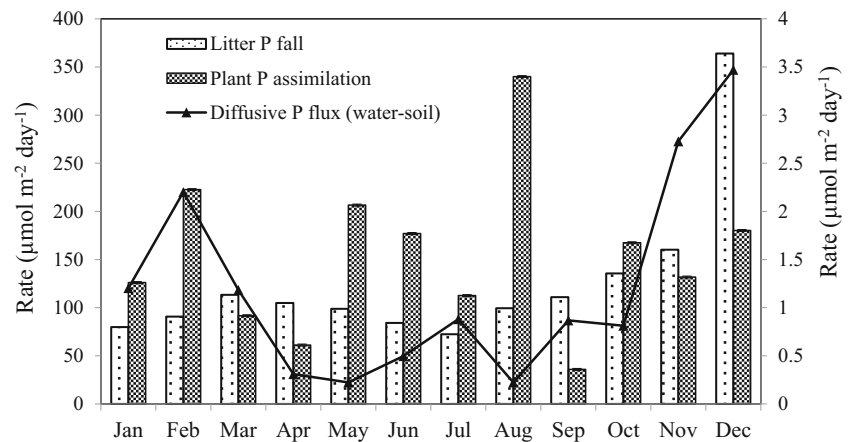
Fig. 5 Monthly variations of P-flux (in 2010) in terms of litter, plant uptake, and diffusive transport

(monsoon) at the river end of the estuary. Tidal variation of mean P concentration in the estuary showed higher values during low tide (LT) than that of high tide (HT) (1.12 μM (monsoon) and 0.82 μM (non-monsoon) versus 0.85 μM (monsoon) and 0.51 μM (non-monsoon)). Seasonal variation of river runoff of P showed maximum value during the monsoon with value of 1.53 Gg which decreased to 0.74 Gg during the non-monsoon period. The salinity gradient ranged from 0.5–1.5 psu at the river end to 30–32 psu at the surface ocean and an intermediate value of 17.9–27 psu at the mid estuary. Since there was quantifiable salinity and P gradient with little stratification ($P = 1.0163–0.019$ S, $r^2 = 0.67$, $P < 0.02$, $n = 10$), this mangrove-dominated estuary was considered suitable for LOICZ modeling. The net residual flows of 1.98 Gg P (LT = 1.11Gg, HT = 0.86) in the monsoon decreased to 0.71 Gg P (LT = 0.42 Gg, HT = 0.29Gg) in the non-monsoon period and the exchange flows of 2.59 Gg P (LT = 1.54 Gg, HT = 1.05 Gg) in the monsoon decreased to 0.73 Gg P (LT = 0.49 Gg, HT = 0.24 Gg) in the non-monsoon period. The net exchange flow (3.3 Gg P) was greater than the residual flow (2.7 Gg P). The annual flux, calculated as the sum of the seasonal fluxes, and total residual and exchange flow (6.0 Gg P year^{-1}) were greater than the river input (2.3 Gg P year^{-1}) resulting net export of 3.7 Gg P year^{-1}.

Aerosol Emission and Dry Deposition of P

The average concentration of PO_4^{3-} in aerosol was found to be 10.01 ± 5.56 μg m^{-3} (November 15.97 μg m^{-3}, December to February 2.59 μg m^{-3}, March to April 10.00 μg m^{-3}, May to June 11.97 μg m^{-3}). The P fluxes emitted to the atmosphere were estimated at 0.002 μg m^{-2} s^{-1} in December to February to 0.14 μg m^{-2} s^{-1} in May to June or 1.4 Gg P year^{-1}. The dry deposition flux of PO_4^{-3} was found to vary between 4.2×10^{-3} to 0.86 μg m^{-2} s^{-1} with an average deposition of 0.32 μg m^{-2} s^{-1} or 5.8 Gg P year^{-1}. The dust deposition flux of PO_4^{-3} ranged from 7.43 mg m^{-2} day^{-1} in February to 55.3 mg m^{-2}day^{-1} in April with an average value of 22.5 ± 18.01 mg m^{-2} day^{-1} or 4.7 Gg P year^{-1}.

Discussion

The study sites were dominated by silty clay-type sedimentary environment (alluvial). In the clay minerals, kaolinite could be associated with quartz, illite, and chlorite (Rajkumar et al. 2012) and the net negative charge, surface area, and porosity of the sediment could play a major role on its adsorption capacity (Alkan et al. 2004).

P in litter (0.12%) compares well with that reported for *Rhizophora* ($0.10 \pm 0.02\%$, Betoulle et al. 2001) and *Kandelia* mangroves (0.14%, Lin and Zheng 1986). Woody residues had the lowest nutrient concentrations in the data set, followed by leaf and roots. The molar C, N, P ratio observed for mangrove litter was consistent composition reported for mangrove litter (1300:33:1, Gordon et al. 1996). Despite relatively low phosphorus concentration among the components of mangrove forest, the C:N and C:P ratios were strongly correlated (C:P = 790 + 8.94 (C:N), $r^2 = 0.66$, $P < 0.01$), indicating that in general sediments are similarly rich in both nutrients and progressive increase of nutrient concentrations from plant residues to sedimentary organic matter. Nutrient mineralization from plant residues is predominantly controlled by the activity of decomposer organisms. Decomposers tend to grow following relatively rigid stoichiometric requirements (Cleveland and Liptzin 2007), and carbon and nutrients are typically processed together in order to achieve balanced growth conditions (Sinsabaugh and Moorhead 1994; Sinsabaugh et al. 2008). The stoichiometric composition of litter can affect the decomposer carbon-use efficiency (e) and it decreases with degree of recalcitrance of organic compounds in litter. Manzoni et al. (2010) proposed a stoichiometric model of litter mineralization, and variability in e was explained by the initial litter $(C:N)_{L0}$ ratio and critical $(C:N)_{CR}$ ratio, as follows:

$$e = 6.25(C:N)_{L0}^{-0.77}$$
$$(C:N)_{CR} = 2.33(C:N)^{0.75}$$

Variability in the P evolution during litter decomposition was also computed by changes in e with residual effect of $(C/P)_B$ and $(C/P)_{CR}$, as follows:

$$(C:P)_B = 14.3(C:P)_{L0}$$
$$(C:P)_{CR} = 2.27(C:P)_{L0}^{0.84}$$

In this study, e and critical C:N and C:P ratios for mangrove litter were found to be 0.31–0.55, 24.5–43, and 681–979, respectively. Since initial C:N (23–49) and C:P (889–1369) in plant residue were high compared to the decomposer requirements (C:N = 8.6–10.1, C:P = 83.6–93.5, Manzoni et al. 2010), nutrients seemed to be initially immobilized from the environment by decomposers. As decomposition proceeded, this difference decreased, as shown clearly by the decreasing trend of sediment plant residue carbon:nutrient ratios (C:N = 14–22; C:P = 81–183, Table 2). When they become lower than the critical level (C:N = 24.5, C:P = 681–979), their net release occurred (Berg and McClaugherty 2003; Moore et al. 2006; Parton et al. 2007). Decomposers showed carbon-use efficiency of 0.86–1.0 for sediment C:N range of 10.6–13 and support the hypothesis that decomposers adapt to low sediment C:N plant residue by enhancing their carbon-use efficiency in mangrove sediment.

A general decrease of both phosphate and PSB with depth (Fig. 2a, b) indicated the presence of phosphate-containing minerals which could be a source of phosphate for PSB in the Sundarban mangrove sediment. Sundby et al. (1992) reported that the non-mobilized phosphorus buried in the accumulating sediment appeared to consist mostly of stable minerals such as apatite, and phosphatase enzyme from those microbes (PSB) solubilized the phosphate-containing minerals (Rodríguez et al. 2006; Rahaman et al. 2013).

Box Model

The basic characteristics of P cycle are often described in terms of the content in the various reservoirs and the fluxes between them (Lerman et al. 1975; Butcher et al. 1992). Box model representation of phosphorus cycle in the Sundarban mangrove system is presented in Fig. 6, in which quantities of P are depicted as uniform within each box, and the flux between them is shown with arrows depending on their net concentrations. There are six coupled reservoirs of P in the model: P in the form of aerosol in the atmosphere, P in the form of organic matter in above- and below-ground biomass, P in the form of organic and inorganic matter in sediment, land estuary and ocean. The fundamental processes involved in the model are as follows: (1) dust aerosol deposition from

the atmosphere and aerosol emission from the forest and surrounding mangrove water, (2) litter from above-ground biomass and roots as below-ground biomass in the sediment, (3) breakdown of plant litter to inorganic P followed by their advective and diffusive exchange between sediment and water, (4) transport of land derive P and deposition of particulate P, (5) out welling of P from the mangrove system to the coastal water.

Phosphate enters the atmosphere from a variety of sources such as continental-derived dust, sea spray, and plant pollen (Mahowald et al. 2005). The net addition of P from atmospheric source (dry deposition of aerosol + dust deposition − emission = 5.8 + 4.73 − 1.36) was found to be 9.17 Gg P year^{-1}. The dust deposition of P (4.73 Gg year^{-1} or 1.11 g m^{-2} year^{-1}) observed in this study was greater than that of Amazon forest (6025×10^9 km^2, Borges et al. 2015). Yu et al. (2015) suggested that dust deposition of P (6–37 Gg P year^{-1} or 1–6 mg m^{-2} year^{-1}) could be attributed to deposition of long range African dust, and Okin et al. (2004) suggested that Amazon rain forests depend on Aeolian deposition for the long-term maintenance of net primary productivity (NPP). Enhanced dust loading (in addition to the locally generated aerosol) transported from the arid and semiarid region of western India and beyond could be responsible for high dust deposition of P over the Sundarban. Continental air masses driven by northeasterly (and easterly) wind flow during winter and northwesterly (and westerly) wind flow passing over Indo-Gangetic plain during pre-monsoon brought dust aerosols over Sundarban (Dey et al. 2004). During this time, due to enhanced convection and steep pressure gradient across the Indo-Gangetic region along with a considerable heat wave running across the region, the dust aerosols were transported from the arid and semiarid regions of western India driven by the pre-monsoon westerlies and mixed up with the natural and anthropogenic aerosols over the Indo-Gangetic basin (Chatterjee et al. 2012).

Forest biomass and sediment-P pool (up to 60 cm depth) was 49.7 Gg P, out of which 97% was in the biomass pool. Litter fall (6.1 Gg P year^{-1}), dry deposition, and riverine input were the major source of phosphorus in the mangrove sediment. Apart from diffusive transport and sedimentation of particulate P (0.78 Gg P year^{-1}) occurred from the estuarine water surrounding mangroves, suggesting role of phytoplankton production (Biswas et al. 2004) to modify the riverine flux of P before it was being released to the coastal water. However, mangrove sediment was a P sink which was consistent with studies in coastal and in particular estuarine sediment (Jonge and de Villerius 1989). Phosphate concentrations of 0.19 to 0.67 µg g^{-1} in the Sundarban mangrove sediment were below its maximum adsorption capacity (Γm = 322.58 µg g^{-1} or 10.4 µmol g^{-1}, Mandal et al. 2011) and were lower than those of tropical forest sediment (6.66–24.9 µmol g^{-1}, Palm et al. 2007), mean marine sediment
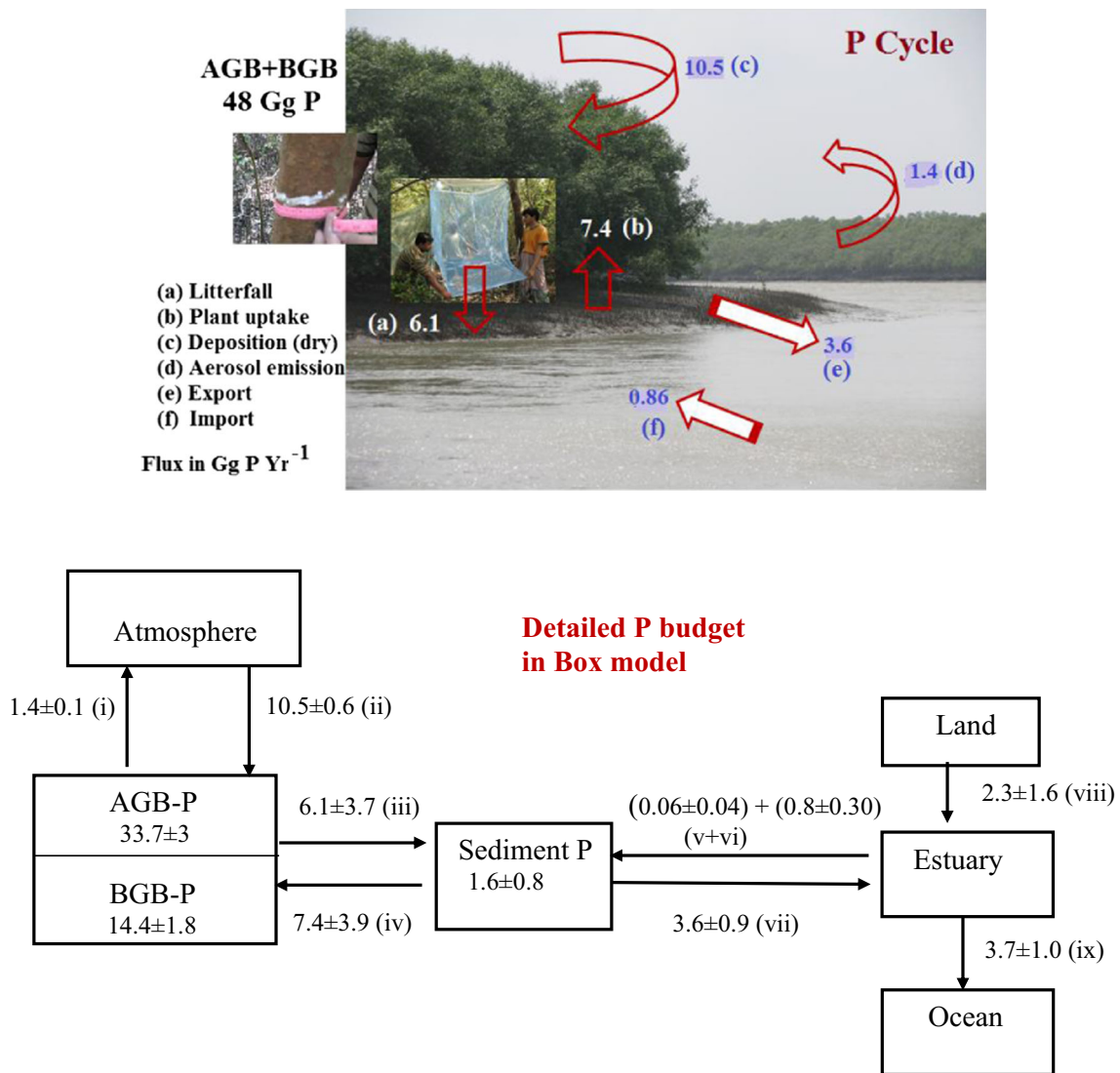
Fig. 6 Photographic overview of P cycle in the Sundarban during the study period. The figure depicts schematic box diagram of P reservoir inventories (unit of stock = Gg P, flux = Gg P year^{-1} mean ± SD) at the Sundarban; (i) aerosol emission, (ii) dry deposition, (iii) litterfall, (iv) plant uptake, (v) diffusive flux, (vi) sedimentation of particulate P flux, (vii) advective flux, (viii) surface runoff, (ix) estuarine export. Areas considered for data upscaling for each fluxes are as follows: (i–v) and (viii) = 4264 km^2; (vi) and (vii) = 1781 km^2

(21.6 μmol g^{-1}, Bowen 1979), and other mangrove sediment (Australian, 3.22–51.6 μmol g^{-1}, Clough et al. 1983). The residence time of P (= total mass of P in reservoir/rate of P removal from reservoir) incorporated into sediment was relatively short (51 days) compared to the mangrove biomass (7.9 year). Major portion of the available nutrients was at all times in the biomass and was recycled within the organic structure of the system and according to Odum's hypothesis (Odum 1971); the pattern of nutrient cycling in the tropics is, in several important ways, different from that in the temperate zone. In cold regions, a large portion of the organic matter and available nutrients is at all times in the soil or sediment; in the tropics, a much larger percentage is in the biomass and is recycled within the organic structure of the system.

The total P flux to the sediment after summing up all sources of P (Gg P year^{-1}), i.e., litter fall (6.1), diffusion (0.06), sedimentation particulate matter (0.8), and net atmospheric deposition (9.1), was 16.06 Gg P year^{-1}. The total removal of P due to plant uptake (7.4 Gg P year^{-1}), advective transport (3.6 Gg P year^{-1}), and export (3.7 Gg P year^{-1} = (V_x + V_R − V_Q)) from mangrove system to coastal water was 14.7 Gg P year^{-1} and plant uptake accounted for 46.1% of the total input. Therefore, the missing P in the budget was 1.36 Gg P year^{-1} or 0.3 g P m^{-2} year^{-1} which corresponds to 8.5% of the total input of P to the Indian Sundarban mangrove system. Pore water advection and/or submarine groundwater discharge (SGD) could enhance benthic fluxes in intertidal flats (Santos et al. 2012). In contrast to nitrogen (N), concentration of P in the pore water was approximately double the tidal water

value and loss of P through sediment pores characterized by advective dispersal was about 62-fold as large as that of dispersal due to molecular diffusion. Pore water advection rate (8.64–11.52 cm day^{-1}) previously estimated by Dutta et al. (2015) and used here for the estimation of advective dispersal of P was very close to the values reported for Waikarea (27 ± 7 cm day^{-1}) and Te Puna (14 ± 5 cm day^{-1}) estuary intertidal flats of New Zealand (Santos et al. 2014). Wang et al. (2014) estimated pore water exchange rate of 13–15 cm day^{-1} into the Sanggou Bay facing Yellow Sea using radon mass balance and showed that SGD-derived DIP flux was 15-fold as large as that of sea water-sediment exchange. Benthic macrofauna-like crabs maintain ecosystem functioning through sediment reworking and consumption of litter, thus reducing detritus available for export and enhancing retention and recycling of nutrients (Kristensen and Alongi 2006; Aschenbroich et al. 2016). Large population of bioirrigators such as tellinid bivalves and crab burrows common in the intertidal flats could drive significant modifications in the sedimentation rate, sediment texture, and surface topography. These could modify pore water flow (Chakraborty and Choudhury 1992; Stieglitz et al. 2000; Li et al. 2009; Santos et al. 2014) and could account missing P in the budget of Sundarban mangrove forest.

Stimulation of terrestrial plant production by rising CO_2 concentration as evidenced by the free-air CO_2 enrichment (FACE) experiments indicated increased NPP of forests by 23 ± 2% in response to atmospheric CO_2 enrichment to 550 ppm (Norby et al. 2005) and was projected to slow the increase in atmospheric CO_2 and the trajectory of climatic warming (Matthews 2007; Denman et al. 2007). However, this negative feedback on atmospheric CO_2 was uncertain because of the expectation that feedbacks through the N and P cycles would reduce this so-called CO_2 fertilization effect (Thornton et al. 2007).

Dynamic Sundarban carbon cycle model (Ray et al. 2013) simulated 1.17- and 2-fold increase of carbon storage in live biomass and sediment, respectively, resulting from the responses of mangroves to atmospheric CO_2 elevated to 580 ppmv. This could increase sequestration of P in long-lived biomass or sediment pools under elevated CO_2, resulting in further decline of P availability in the tight P budget of Sundarban, and could induce a negative feedback further on mangrove productivity increase under elevated CO_2.

Conclusion

A reservoir-based mass budget of phosphorus has been constructed for the Indian Sundarban mangroves considering live and sedimentary stocks and biogeochemical fluxes operating within the ecosystem. This is the first comprehensive study on

P cycle for the region and the major conclusions drawn from this study are as follows:

(a) Despite relatively low phosphorus concentration among the components of mangrove forest, the C:N and C:P ratios are strongly correlated and the major fraction of the available P in the Sundarban mangrove ecosystem is at all times in the biomass and is recycled within the organic structure of the system.

(b) The interactions of C, N, and P play important roles in regulating the availability of P and carbon uptake and storage, suggesting that the Sundarban mangrove ecosystem responses to increasing atmospheric $[CO_2]$ will interact strongly with changes in the P cycle.

(c) The input of P from fallout from dust and biochemical mineralization of organic P can significantly affect P availability and determine the extent of P limitation in Sundarban mangrove forest under elevated atmospheric CO_2.

References

Alkan, M., O. Demirbas, S. Celikcapa, and M. Dogan. 2004. Sorption of acid red 57 from aqueous solutions onto sepiolite. *Journal of Hazardous Materials* 116: 135–145.

Alongi, D.M. 2009. *The energetics of mangrove forests*, 216. Dordrecht: Springer.

Alongi, D.M., K.G. Boto, and F. Tirendi. 1989. Effect of exported mangrove litter on bacterialproductivity and dissolved organic carbon fluxes in adjacent tropical nearshore sediments. *Marine Ecology Progress Series* 56: 1331–1144.

Alongi, D.M., K.G. Boto, and A.I. Robertson. 1992. Nitrogen and phosphorous cycles. In *Tropical mangrove ecosystems*, ed. A.I. Robertson and D.M. Alongi, 251–292. Washington, DC: American Geophysical Union (AGU).

APHA 20005. 1995. *Standard methods for the examination of water and waste water*. Washington, pp. 5–15.

Aschenbroich, A., E. Michaud, T. Stieglitz, F. Fromard, A. Gardel, M. Tavares, and G. Thouzeau. 2016. Brachyuran crab community structure and associated sediment reworking activities in pioneer and young mangroves of French Guiana, South America. *Estuarine Coastal Shelf Science* 182: 60–71.

Banerjee, K., B. Senthilkumar, R. Purvaja, and R. Ramesh. 2011. Sedimentation and trace metal distribution in selected locations of Sundarbans mangroves and Hooghly estuary, northeast coast of India. *Environmental Geochemical Health* 34: 27–42.

Berg, B., and C.A. McClaugherty. 2003. *Plant litter: decomposition, humus formation, carbon sequestration*. Berlin: Springer.

Berner, R.A. 1980. *Early diagenesis: a theoretical approach*. Princeton: Princeton University Press.

Betoulle, J.L., F. Fromard, F. André, and P. Henri. 2001. Caractérisation des chutes de litière et des apports au sol en nutriments dans une mangrove de Guyane française. *Canadian Journal of Botany* 79: 238–249.

Biswas, H., S.K. Mukhopadhyay, T.K. De, S. Sen, and T.K. Jana. 2004. Biogenic controls on the air—water carbon dioxide exchange in the Sundarban mangrove environment, northeast coast of Bay of Bengal, India. *Limnology and Oceanography* 49: 95–101.

Borges, A.V., G. Abril, F. Darchambeau, C.R. Teodoru, J. Deborde, L.O. Vidal, T. Lambert, and S. Bouillon. 2015. Divergent biophysical controls of aquatic CO_2 and CH_4 in the World's two largest rivers. *Scientific Reports* 5: 15614. https://doi.org/10.1038/srep15614.

Bowen, H.J.M., 1979. Environmental Chemistry of the Elements. Academic Press, London

Branom, J.R., and D. Sarkar. 2004. Phosphorus bioavailability in sediments of a sludge-disposal lake. *Environmental Geosciences* 11: 42–52.

Butcher, S.S., R.J. Charlson, G.H. Orians, and G.V. Wolfe. 1992. *Global biogeochemical cycles*. London: Academic Press.

Chakraborty, S.K., and A. Choudhury. 1992. Population ecology of fiddler crabs (Uca spp.) of the mangrove estuarine complex of Sundarbans, India. *Tropical Ecology* 33: 78–88.

Chang, S.C., and M.L. Jackson. 1957. Fractionation of soil phosphorus. *Soil Science* 84: 133–144.

Chatterjee, A., C. Dutta, S. Sen, K. Ghosh, N. Biswas, D. Ganguly, and T.K. Jana. 2006. Formation, transformation, and removal of aerosol over a tropical mangrove forest. *Journal of Geophysical Research* 111: D24302. https://doi.org/10.1029/2006JD007144.

Chatterjee, A., C. Dutta, T.K. Jana, and S. Sen. 2012. Fine mode aerosol chemistry over a tropical urban atmosphere: characterization of ionic and carbonaceous species. *Journal of Atmospheric Chemistry* 69: 83–100.

Chowdhury, C., N. Majumder, R. Ray, and T.K. Jana. 2012. Inter-annual variation in some genera of diatom and zooplankton in a mangrove ecosystem. *Biodiversity and Conservation* 21: 2029–2043.

Christian, G.D. 2001. *Analytical chemistry*. Fifth ed. Singapore: Wiley.

Clark, D.A., S. Brown, D.W. Kicklighter, J.Q. Chambers, J.R. Thomlinson, J. Ni, and E.A. Holland. 2001. Net primary production in tropical forests: an evaluation and synthesis of existing field data. *Ecological Applications* 11: 371–384.

Cleveland, C.C., and D. Liptzin. 2007. C:N:P stoichiometry in soil: Is there a "Redfield ratio" for the microbial biomass? *Biogeochemistry* 85: 235–252.

Clough, B.F., K.G. Boto, and P.M. Attiwill. 1983. Mangrove and sewage: a re-evaluation. In *Biology and ecology of mangroves*, ed. H.J. Teas , 151–162. Lancaster: Dr W. Junk Publishers.Tasks for Vegetation Science Series

Conley, D.J., H.W. Paerl, R.W. Howarth, D.F. Boesch, S.P. Seitzinger, K.E. Havens, C. Lancelot, and G.E. Likens. 2009. Controlling eutrophication: nitrogen and phosphorus. *Science* 323: 1014–1015.

Cross, A.E., and W.H. Schlesinger. 1995. A literature review and evaluation of the Hedley fractionation: applications to the biogeochemical cycle of soil phosphoms in natural ecosystems. *Geoderma* 64: 197–214.

Das, S., T.K. De, and T.K. Jana. 2014. Vertical profile of phosphatase activity in the Sundarban mangrove forest, North East Coast of Bay of Bengal, India. *Geomicrobiology Journal* 31: 716–725.

Denman, K.L., et al. 2007. Climate change 2007: the physical science basis. In *Contribution of working group I to the fourth assessment report of the intergovernmental panel on climate change*, ed. S.D. Solomon et al., 499–587. Cambridge), Chap 7: Cambridge University Press.

Dey, S., S.N. Tripathi, R.P. Singh, and B.N. Holben. 2004. Influence of dust storms on the aerosol optical properties over the Indo-Gangetic

Basin. *Journal of Geophysical Research* 109: D20211. https://doi.org/10.1029/2004JD004924.

Dey, M., D. Ganguly, C. Chowdhury, N. Majumder, and T.K. Jana. 2012. Intra-annual variation of modern foraminiferal assemblage in a tropical mangrove ecosystem in India. *Wetlands* 32: 813–826.

Dick, W.A., L. Cheng, and P. Wang. 2000. Soil acid and alkaline phosphatase activity as pH adjustment indicators. *Soil Biology & Biochemistry* 32: 1915–1919.

Dittmar, T., and R.J. Lara. 2001. Do mangroves rather than rivers provide nutrients to coastal environments south of the Amazon River? Evidence from long-term flux measurements. *Marine Ecology Progress Series* 213: 67–77.

Donato, D.C., J.B. Kauffman, D. Murdiyarso, S. Kurnianto, M. Stidham, and M. Kanninen. 2011. Mangroves among the most carbon-rich forests in the tropics. *Nature Geoscience* 4: 293–297.

Dutta, M.K., R. Mukherjee, T.K. Jana, and S.K. Mukhopadhyay. 2015. Biogeochemical dynamics of exogenous methane in an estuary associated to a mangrove biosphere; the Sundarbans, NE coast of India. *Marine Chemistry* 170: 1–10.

FAO 2004. Status and trends in mangrove area extent worldwide. Forest Resources Assessment Working Paper; 063–287.

Feller, I.C., C.E. Lovelock, U. Berger, K.L. McKee, S.B. Joye, and M.C. Ball. 2010. Biocomplexity in mangrove ecosystems. *Annual Review of Marine Science* 2: 395–417.

Fiedler, S., G.U. Scholich, and M. Kleber, 2003. Innovative electrode design helps to use redox potential as a predictor for methane emissions from soils. Communications in Soil Science and Plant Analysis 34: 481–496.

Gerretsen, F.C. 1948. The influence of microorganisms on the phosphate intake by the plant. *Plant and Soil* 1: 51–81.

Gifford, F.A., and S.R. Hanna. 1973. Modelling urban air pollution. *Atmospheric Environment* 7: 131–136.

Gordon Jr. D.C., P.R. Boudreau, K.H. Mann, J-E. Ong, W.L. SIlvert, S.V. Smith, G. Wattayakorn, F. Wulff, and T. Yanagi. 1996. LOICZ biogeochemical modelling guidelines. *LOICZ reports and studies* No. 5, pp. 51.

Graedel, T.E., and P.J. Crutzen. 1993. *Atmospheric change*, 83. New York: W. H. Freeman & Company.

Grasshoff, K. 1983. Determination of salinity and oxygen, determination of nutrients. In *Methods of seawater analysis*, ed. K. Grasshoff, M. Ehrhard, and K. Kremling, 31–125. Weinheim: Verlag Chemie.

Holguin, G., P. Vazavez, and Y. Bahon. 2001. The role of sediment microorganism in the productivity, conservation and rehabilation of mangrove ecosystems: an overview. *Biology and Fertility of Soils* 33: 265–278.

Hussein, M.Z. 1995. Silviculture of mangroves. *Unasylva* 46: 36–42.

Iversen, N., and B.B. Jorgensen. 1993. Diffusion coefficients of sulphate and methane in marine sediments : influence of porosity. *Geochimica Cosmochimica Acta* 57: 571–578.

Johnson, R.A., J. Erizano, and D.R. Vann. 2003. Biogeochemical implications of labile phosphorus in forest soils determined by the Hedley fractionation procedure. *Oecologia* 135: 487–499.

Jonge, V.N., and L.A. de Villerius. 1989. Possible role of carbonate dissolution in estuarine phosphate dynamics. *Limnology and Oceanography* 34: 332–340.

Kelleher, G., C. Bleakley, and S. Wells. 1995. *A global representative system of marine protected areas. 1.* Washington DC: World Bank.

Knab, N.J., B.A. Cragg, E.R.C. Hornibrook, L. Holmkvist, R.D. Pancost, C. Borowski, R.J. Parkes, and B.B. Jørgensen. 2009. Regulation of anaerobic methane oxidation in sediments of the Black Sea. *Biogeosciences* 6: 1505–1518.

Kothamasi, D., S. Kothamasi, A. Bhattacharyya, R. Kuhad, and C. Babu. 2006. Arbuscular mycorrhizae and phosphate solubilising bacteria of the rhizosphere of the mangrove ecosystem of Great Nicobar island, India. *Biology and Fertility of Soils* 42: 358–361.

Kristensen, E., and D.M. Alongi. 2006. Control by fiddler crabs (Uca vocans) and plant roots (Avicennia marina) on carbon, iron, and sulfur biogeochemistry in mangrove sediment. *Limnology and Oceanography* 51: 1557–1571.

Lerman, A., F.T. MacKenzie, and R.M. Garrels. 1975. Modeling of geochemical cycles: phosphorus as an example. *Geological Society of America* 142: 205–218.

Li, X., B.X. Hu, W.C. Burnett, I.R. Santos, and J.P. Chanton. 2009. Submarine groundwater discharge driven by tidal pumping in a heterogeneous aquifer. *Ground Water* 47: 558–568.

Lin, P., and W.J. Zheng. 1986. Studies on the increments of two mangrove species, *Kandelia candel* (L.) Druce and Bruguiera sex angular (Lour.) Poir., in China. *Acta Botanica Sinica* 28: 224–228.

Lovelock, C.E., I.C. Feller, K.L. Mc Kee, and R. Thompson. 2005. Variation in mangrove forest structure and sediment characteristics in Bolas del Toro, Panama. *Caribbean Journal of Science* 41: 456–464.

Lovelock, C.E., I.C. Feller, M.C. Ball, J. Ellis, and B. Sorrell. 2007. Testing the growth rate vs. geochemical hypothesis for latitudinal variation in plant nutrients. *Ecology Letters* 10: 1154–1163.

Mahowald, N.M., P. Artaxo, A.R. Baker, T.D. Jickells, G.S. Okin, J.T. Randerson, and A.R. Townsend. 2005. Impacts of biomass burning emissions and land use change on Amazonian atmospheric phosphorus cycling and deposition. *Global Biogeochemical Cycles* 19: GB4030. https://doi.org/10.1029/2005GB002541.

Mandal, S.K., N. Majumder, C. Chowdhury, D. Ganguly, M. Dey, and T.K. Jana. 2011. Adsorption kinetic control of As (III & V) mobilization and sequestration by mangrove sediment. *Environmental Earth Science* 65: 2027–2036.

Manzoni, S., J.A. Trofymow, R.B. Jackson, and A. Porporato. 2010. Stoichiometric controls on carbon, nitrogen, and phosphorus dynamics in decomposing litter. *Ecological Monographs* 80: 89–106.

Matthews, H.D. 2007. Implications of CO_2 fertilization for future climate change in a coupled climate-carbon model. *Global Change Biology* 13: 1068–1078.

McGrath, D.A., C.K. Smith, H.L. Gholz, and E.D. Oliveira. 2001. Effects of land-use change on soil nutrient dynamics in Amazonia. *Ecosystems* 4: 625–645.

Moore, T.R., J.A. Trofymow, C.E. Prescott, J. Fyles, and B.D. Titus. 2006. Patterns of carbon, nitrogen and phosphorus dynamics in decomposing foliar litter in Canadian forests. *Ecosystems* 9: 46–62.

Mukhopadhyay, S.K., H. Biswas, T.K. De, and T.K. Jana. 2006. Fluxes of nutrients from the tropical River Hooghly at the land–ocean boundary of Sundarbans, NE Coast of Bay of Bengal, India. *Journal of Marine Systems* 62: 9–21.

Norby, R.J., E.H. Delucia, B. Gielen, C. Calfapietra, C.P. Giardina, et al. 2005. Forest response to elevated CO_2 is conserved across a broad range of productivity. *Proceedings of the Natural Academy of Sciences* 102: 18052–18056.

Oberson, A., D.K. Friesen, I.M. Rao, S. Bühler, and E. Frossard. 2001. Phosphorus trans-formations in an oxisol under contrasting land-use systems: the role of the soil microbial biomass. *Plant and Soil* 237: 197–210.

Odum, E.P. 1971. *Fundamentals of ecology*. 3rd ed. London: W. B. Saunders Company.

Oehl, F., A. Oberson, M. Probst, A. Fliessbach, H.R. Roth, and E. Frossard. 2001. Kinetics of microbial phosphorus uptake in cultivated soils. *Biology and Fertility of Soils* 34: 32–41.

Oelkers, E.H. 2008. Phosphate mineral reactivity: from global cycles to sustainable development. *Mineralogical Magazine* 72: 337–340.

Okin, G.S., N. Mahowald, O.A. Chadwick, and P. Artaxo. 2004. Impact of desert dust on the biogeochemistry of phosphorus in terrestrial ecosystems. *Global Biogeochemical Cycles* 18: GB2005. https://doi.org/10.1029/2003GB002145.

Palm, C., P. Sanchez, S. Ahamed, and A. Awiti. 2007. Soils: a contemporary perspective. *Annual Review of Environment and Resources* 32: 99–129.

Parton, W., W.L. Silver, I.C. Burke, L. Grassens, M.E. Harmon, W.S. Currie, J.Y. King, E.C. Adair, L.A. Brandt, S.C. Hart, and B. Fasth. 2007. Global-scale similarities in nitrogen release patterns during long-term decomposition. *Science* 315: 361–364.

Pasquill, F., and F.B. Smith. 1983. *Atmospheric diffusion*, 309–358. New York: Halsted.

Peltzer, D.A., et al. 2010. Understanding ecosystem retrogression. *Ecological Monographs* 80: 509–529.

Piper, C.S. 1950. *Soil and plant analysis*. New York: Inter Science Publishers.

Primavera, J.H. 1997. Socio-economic impacts of shrimp culture. *Aquatic Research* 28: 815–827.

Rahaman, S.M.B., L. Sarder, M.S. Rahaman, A.K. Ghosh, S.K. Biswas, S.M.S. Siraj, A.K. Huq, A.F. Md Hasanuzzaman, and S.S. Islam. 2013. Nutrient dynamics in the Sundarban mangrove estuarine system of Bangladesh under different weather and tidal cycles. *Ecological Processes* 2: 29. https://doi.org/10.1186/2192-1709-2-29.

Rajkumar, K., A.L. Ramanathan, and P.N. Behera. 2012. Characterization of clay minerals in the Sunda, Mangrove River sediments by SEM/EDS. *Journal of Geological Society of India* 80: 429–434.

Ramanathan, A.L., G. Singh, J. Majumder, A.C. Samal, R. Chowhan, R.K. Rayan, K. Roykumar, and S.C. Santra. 2008. A study of microbial diversity and its interaction with nutrients in the sediments of Sundarban mangroves. *Indian Journal of Marine Science* 37: 159–165.

Ramos, E., C.A. Silva, S.R. Oliveira, R.D.P. Regoand, and A.A. Mozeto. 2007. Dynamics of phosphorus and nitrogen through litter fall and decomposition in a tropical mangrove forest. *Marine Environmental Research* 64: 524–534.

Ray, R., D. Ganguly, C. Chowdhury, M. Dey, S. Das, M.K. Dutta, S.K. Mandal, N. Majumder, T.K. De, S.K. Mukhopadhyay, and T.K. Jana. 2011. Carbon sequestration and annual increase of carbon stock in a mangrove forest. *Atmospheric Environment* 45: 5016–5024.

Ray, R., C. Chowdhury, N. Majumdar, M.K. Dutta, S.K. Mukhopadhyay, and T.K. Jana. 2013. Improved model calculation of atmospheric CO_2 increment in affecting carbon stock of tropical mangrove forest. *Tellus B: Chemical and Physical Meteorology* 65: 18981.

Ray, R., N. Majumder, S. Das, C. Chowdhury, and T.K. Jana. 2014. Biogeochemical cycle of nitrogen in a tropical mangrove ecosystem, east coast of India. *Marine Chemistry* 167: 33–43.

Reay, W.G., D. Gallagher, and G.M. Simmons. 1995. Sediment water column nutrient exchanges in Southern Chesapeake Bay near shore environments. Virginia Water Resources Research Centre, Bulletin - 181b.

Reef, R., I.C. Feller, and C.E. Lovelock. 2010. Nutrition of mangroves. *Tree Physiology* 30: 1148–1160.

Reich, P.B., and J. Oleksyn. 2004. Global patterns of plant leaf N and P in relation to temperature and latitude. *Proceedings of the Natural Academy of Sciences* 101: 11001–11006.

Stieglitz, T., P. Ridd, and P. Muller. 2000. Passive irrigation and functional morphology of crustacean burrows in a tropical mangrove swamp. *Hydrobiologia* 421: 69–76.

Rodriiguez, H., R. Fraga, T. Gonzalez, and Y. Bashan. 2006. Genetics of phosphate solubilization and its potential applications for improving plant growth-promoting bacteria. *Plant and Soil* 287: 15–21.

Ruttenberg, K.C. 1992. Development of a sequential extraction method for different forms of phosphorus in marine sediments. *Limnology and Oceanography* 37: 1460–1482.

Sanchez, P.A. 1977. Properties and management of soils in the tropics. *Soil Science* 124: 187.

Santos, I.R., B.D. Eyre, and M. Huettel. 2012. The driving forces of porewater and groundwater flow in the permeable coastal sediments: a review. *Estuarine Coastal Shelf Science* 98: 1–15.

Santos, I.R., K.R. Bryan, C.A. Pilditch, and D.R. Tait. 2014. Influence of porewater exchange on nutrient dynamics in two New Zealand estuarine intertidal flats. *Marine Chemistry* 167: 57–70.

Schelde, K., et al. 2006. Effects of manure application and plowing on transport of colloids and phosphorus to tile drains. *Vadose Zone Journal* 5: 445–458.

Sehmel, G.A., and W.H. Hodgson. 1978. *A model for predicting dry deposition of particles and gases to environmental surfaces, PNL-SA-6721 (and in revised form October 1979, PNL-SA-6721-REV-1), Battelle*. Richland: Pacific Northwest Lab.

Singh, G., R. Chauhan, R.K. Ranjan, M. Balakrishna Prasad, and A.L. Ramanathan. 2015. Phosphorus dynamics in mangroves of India. *Current Science* 108: 1874–1881.

Sinsabaugh, R.L., and D.L. Moorhead. 1994. Resource allocation to extracellular enzyme production: a model for nitrogen and phosphorus control of litter decomposition. *Soil Biology & Biochemistry* 26: 1305–1311.

Sinsabaugh, R.L., et al. 2008. Stoichiometry of soil enzyme activity at global scale. *Ecology Letters* 11: 1252–1264.

Spalding, M., F. Blasco, and C. Field. 1997. *World mangrove atlas*. Okinawa: International Society for Mangrove Ecosystems.

Sturgeon, R.E., J.A.H. Desaulniers, S.S. Berman, and D.S. Russel. 1982. Determination of trace metals in estuarine sediments by graphite-furn aceatomic absorption spectromatry. *Analytica Chimica Acta* 134: 283–291.

Sundby, B., C. Gobeil, N. Silverberg, and A. Mucci. 1992. The phosphorus cycle in coastal marine sediments. *Limnology and Oceanography* 37: 1129–1145.

Terchunian, A., V. Klemas, A. Alvarez, B. Vasconez, and L. Guerrero. 1986. Mangrove mapping in Ecuador: the impact of shrimp pond construction. *Environment Management* 10: 345–350.

Thornton, P.E., J.F. Lamarque, N.A. Rosenbloom, and N.M. Mahowald. 2007. Influence of carbon-nitrogen cycle coupling on land model response to CO2 fertilization and climate variability. *Global Biogeochemical Cycles* 21: GB4018.

Valiela, I., J.L. Bowen, and J.K. York. 2001. Mangrove forests: one of the world's threatened major tropical environments. *Bioscience* 51: 807–815.

Vazquez, P., G. Holguin, M.E. Puente, A. Lopez-Cortes, and Y. Bashan. 2000. Phosphate-solubilizing microorganisms associated with the rhizosphere of mangroves in a semiarid coastal lagoon. *Biology and Fertility Soils* 30: 460–468.

Vischer, P.T., J. Beukema, and H. van Gemerden, 1991. In situ characterization of sediments: measurements of oxygen and sulfide profileswith a novel combined needle electrode. Limnology and Oceanography 36: 1476–1480.

Wang, X., J. Du, T. Ji, T. Wen, S. Liu, and J. Zhang. 2014. An estimation of nutrient fluxes via submarine groundwater discharge into the Sanggou Bay—a typical multi-species culture ecosystem in China. *Marine Chemistry* 167: 113–122.

Wolanski, E. 1992. Hydrodynamics of tropical coastal marine systems. In *Pollution in tropical aquatic systems*, ed. D. Connell and D. Hawker, 3–27. Boca Raton: CRC.

Wright, S.J., J.B. Yavitt, N. Wurzburger, B.L. Turner, E.V. Tanner, E.J. Sayer, L.S. Santiago, M. Kaspari, L.O. Hedin, and K.E. Harms. 2011. Potassium, phosphorus, or nitrogen limit root allocation, tree growth, or litter production in a lowland tropical forest. *Ecology* 92: 1616–1625.

Yang, X., and W.M. Post. 2011. Phosphorus transformations as a function of pedogenesis: a synthesis of soil phosphorus data using Hedley fractionation method. *Biogeosciences* 8: 907–291.

Yang, X., P.E. Thornton, D.M. Ricciuto, and W.M. Post. 2014. The role of phosphorus dynamics in tropical forests—a modeling study using CLM-CNP. *Biogeosciences* 11: 1667–1681.

Yu, H.B., M. Chin, H.S. Bian, T.L. Yuan, J.M. Prospero, A.H. Omar, L.A. Remer, D.M. Winker, Y.K. Yang, Y. Zhang, and Z.B. Zhang. 2015. Quantification of trans-Atlantic dust transport from seven-year (2007–2013) record of CALIPSO lidar measurements. *Remote Sensing of Environment* 159: 232–249.